Characteristic submucosal alteration in biliary carcinogenesis of pancreaticobiliary maljunction with a focus on inflammasome activation

Shoko Yamashita[1,2], Chie Takasu[1], Yuji Morine[1], Hiroki Ishibashi[1], Tetsuya Ikemoto[1], Hiroki Mori[1], Shinichiro Yamada[1], Takeshi Oya[3], Koichi Tsuneyama[2], and Mitsuo Shimada[1]

[1]Department of Surgery, Tokushima University, Kuramoto-cho, Tokushima 770-8503, Japan

[2]Department of Pathology and Laboratory Medicine, Tokushima University, Kuramoto-cho, Tokushima 770-8503, Japan

[3]Department of Molecular Pathology, Tokushima University, Kuramoto-cho, Tokushima 770-8503, Japan

Word count of abstract: 193

Word count of abstract + main text: 3,751

Number of figures and tables: 7 figures and 0 tables

Correspondence to:

Yuji Morine, MD, PhD

Department of Surgery, Institute of Biomedical Sciences, Tokushima University Graduate School, 3-18-15 Kuramoto-cho, Tokushima 770-8503, Japan

Tel: +81-88-633-9276

Fax: +81-88-631-9698

E-mail: **ymorine@tokushima-u.ac.jp**

ABSTRACT

Background

This study investigated submucosal alterations in biliary carcinogenesis of pancreaticobiliary maljunction (PBM).

Methods

Thirty-three patients with PBM (including seven with gallbladder [GB] cancer), four with neither biliary tract cancer nor PBM who underwent pancreaticoduodenectomy (controls), and seven with chronic cholecystitis without PBM were enrolled. Protein expression of α-smooth muscle actin (αSMA), CD68, and CD204 in the GB lamina propria and that of NLRP3 and caspase 1 in the GB epithelium and lamina propria were examined.

Results

Compared with the control and cholecystitis groups, αSMA expression was higher in the cancerous part (stroma) of the GB in patients with GB cancer + PBM and in the lamina propria of patients with PBM. The CD204/CD68 ratio in the lamina propria was higher in the PBM group than in the control and cholecystitis groups. NLRP3 and caspase 1 expression in both the lamina propria and epithelium was higher in the PBM

than control group. In the PBM group, NLRP3- and caspase 1-positive cells in the lamina propria were located near the epithelium.

Conclusion

Activated fibroblasts and M2 macrophages in the GB lamina propria may be associated with biliary carcinogenesis of PBM, possibly through inflammasome activation.

Keywords

Biliary cancer, activated fibroblast, M2 macrophage, NLRP3, caspase 1

Abbreviations

PBM: pancreaticobiliary maljunction

GB: gallbladder

TAM: tumor-associated macrophage

CAF: cancer-associated fibroblast

TME: tumor microenvironment

αSMA: α-smooth muscle actin

NLRP3: Nod-like receptor pyrin domain containing 3

PBS: phosphate-buffered saline

IL: interleukin

DAMPs: damage-associated molecular patterns

INTRODUCTION

Pancreaticobiliary maljunction (PBM) is defined as abnormal union of the biliopancreatic ducts. PBM is a risk factor for biliary cancer, and the occurrence rate of PBM-associated biliary cancer is much higher than that of biliary cancer without PBM [1]. The mechanism underlying biliary carcinogenesis of PBM has been linked to the stagnation of bile mixed with pancreatic juice in the bile duct and gallbladder (GB). Studies of PBM-associated carcinogenesis have revealed *K-ras* and *p53* gene mutations in epithelial cells of the GB [2]. In patients with PBM, the sequence of hyperplasia–dysplasia–carcinoma is regarded as the prevailing mechanism underlying the development of biliary cancer. Research has shown that the mechanism of biliary carcinogenesis of PBM involves only changes in the biliary epithelium. However, the carcinogenic alteration in the lamina propria of the GB in patients with PBM remains unknown.

Tumor-associated macrophages (TAMs) and cancer-associated fibroblasts (CAFs) in the tumor microenvironment (TME) promote the malignancy of cancer cells and therapeutic resistance of multiple cancer types. CAFs are an activated form of fibroblasts and are distinct from fibroblasts in their expression of α-smooth muscle actin

(SMA) [3-5]. Macrophages are classified into two types: 1) the classically activated, proinflammatory M1 macrophage and 2) the alternatively activated, anti-inflammatory M2 macrophage. M2 macrophages exhibit low antigen presentation efficiency and produce high levels of anti-inflammatory cytokines [3-5]. TAMs exhibit characteristics similar to those of M2 macrophages and are characterized by M2 macrophage-specific markers such as CD163 and CD204 [5]. The relationship between stromal changes and carcinogenesis has been the subject of investigation in several types of cancer. M2 macrophage infiltration has been observed in the submucosal tissue of ulcerative colitis and human papillomavirus-infected cervical cells [6, 7]. Crosstalk between senescent breast cells and activated fibroblasts contributes to the carcinogenesis of breast cancer [8]. However, no study has been performed to examine the influence of M2 macrophages and activated fibroblasts on PBM carcinogenesis.

Nod-like receptor pyrin domain containing 3 (NLRP3), a member of the NLR protein family, is an important component of the inflammasome [9]. Furthermore, NLRP3 may play a pathological role in tumorigenesis by its modulation of innate and adaptive immunity, apoptosis, and differentiation [9-11]. We hypothesized that NLRP3 is a major molecule in PBM-associated carcinogenesis because NLRP3 is a major component of

inflammatory carcinogenesis. However, to the best of our knowledge no study has been performed to examine NLRP3 expression in patients with PBM.

In this study, we investigated both the epithelium and lamina propria of the GB to elucidate the mechanism of biliary carcinogenesis of PBM by focusing on activated fibroblasts, M2 macrophages, and inflammasome activation.

MATERIAL AND METHODS

Patient selection

This study involved a total of 44 patients. The PBM group comprised 33 patients with PBM who underwent either total excision of the extrahepatic biliary tract (including the GB) combined with biliary reconstruction or cholecystectomy alone from 1992 to 2020. Of these 33 patients, 7 had PBM-associated GB cancer. Among these seven patients with PBM-associated GB cancer, four had only cancerous tissue in the surgical specimens for immunostaining, whereas three had both cancerous tissue and non-cancerous tissue. The control group comprised four patients with neither biliary tract cancer nor PBM who underwent pancreaticoduodenectomy. Finally, the cholecystitis group comprised seven patients with chronic cholecystitis who were selected as representative cases of simple biliary inflammation without PBM. Immunohistochemical staining of the GB was performed in the above all patients. This study was approved by the Ethics Committee of Tokushima University (TOCMS ID: 3010-1).

Immunohistochemical staining and assessment

Immunohistochemical staining was performed as previously described [12]. Briefly, 4-μm-thick tissue sections from each sample were deparaffinized and dehydrated. The sections were treated with 0.3% hydrogen peroxide and methanol for 20 minutes to halt peroxidase activity, and this was followed by heat treatment. The sections were then incubated overnight at 4°C with a primary mouse monoclonal antibody to αSMA (ab7817, 1:100 dilution in phosphate-buffered saline [PBS]; Abcam, Cambridge, UK) and primary rabbit polyclonal antibodies to NLRP3 (ab214185, 1:200 dilution in PBS; Abcam) and caspase 1 (GTX101322, 1:100 dilution in PBS; Genetex, Irvine, CA, USA). Finally, the sections were treated with a secondary antibody (EnVision™+ Dual Link System-HRP; Dako, Glostrup, Denmark) for 1 hour at room temperature.

To evaluate CAFs, the samples were analyzed using 200× magnification. The area fraction of CAFs was defined as the ratio of the αSMA-positive area to the total area on the microscopic field, determined using ImageJ software version 1.53a (National Institutes of Health, Bethesda, MD, USA) [5].

To evaluate NLRP3 and caspase 1 expression in the GB epithelium, the H-score was determined for each sample [10]. The H-score was calculated by multiplying

the staining percentage (0%–100%) by the staining intensity (1: weak, 2: moderate, and 3: strong), with a score ranging from 0 to 300 [10]. In accordance with the NLRP3 and caspase 1 expression in the lamina propria of the GB, as reported previously, spindle-shaped non-neoplastic cells (excluding macrophages and lymphocyte-like round cells) were recognized as fibroblasts, and cytoplasmic expression of NLRP3 and caspase 1 in these cells was considered positive [11, 12]. Cells positive for NLRP3 and caspase 1 were identified by screening the entire area in a low-power (100×) field and selecting the three areas with the highest density of stained cells. The mean number of positive cells in three independent high-power (400×) fields was calculated.

All immunostained sections were evaluated by a pathologist blinded to the patients' information.

Immunofluorescence staining

Immunofluorescence staining was performed as previously reported [3]. The primary antibodies were rabbit polyclonal antibodies to CD204 (TK022, 1:50 dilution in PBS; TransGenic Inc., Kobe, Japan), CD68 (ab955, 1:100 dilution in PBS; Abcam), NLRP3 (NBP2-12446, 1:50 dilution in PBS; Novus Biologicals LLC, Centennial, CO,

USA), caspase 1 (NBP2-12446, 1:500 dilution in PBS; Genetex), and αSMA (ab7817, 1:100 dilution in PBS; Abcam). The secondary antibodies were anti-rabbit Alexa 488 (1:500, A-11008; Life Technologies, Carlsbad, CA, USA) and anti-mouse Alexa 594 (1:500, A-11005; Life Technologies).

For CD204 and CD68 double staining, a dual immunofluorescence method was used as previously described [13] with some modifications. Briefly, the sections were incubated overnight with the anti-CD68 antibody at 4°C. They were then incubated with Alexa 594 anti-mouse IgG as the secondary antibody for 1 hour and then blocked with 5% mouse serum and 5% anti-mouse IgG Fab (Jackson ImmunoResearch Laboratories, West Grove, PA, USA) for 1 hour each. Next, the sections were incubated with the anti-CD204 antibody overnight at 4°C, followed by Alexa 488 anti-mouse IgG for 1 hour. Expression was determined by analyzing three randomly selected fields at high magnification (×400) [14].

Statistical analysis

All statistical analyses were performed using statistical software (JMP 11.2.0; SAS Institute, Cary, NC, USA). Comparisons of several parameters were analyzed with

one-way analysis of variance followed by Bonferroni's post-hoc correction. Statistical significance was defined as $P < 0.05$.

RESULTS

Activated fibroblasts and M2 macrophages in the lamina propria of the GB in patients with PBM

To examine the significance of activated fibroblasts and M2 macrophages in biliary carcinogenesis of PBM, we performed immunohistochemical staining of αSMA and dual immunofluorescence staining of CD68 and CD204. Immunohistochemical staining of GB tissues from patients with PBM revealed spindle-shaped cells expressing αSMA in addition to vascular smooth muscle cells (Figure 1). Dual immunofluorescence staining revealed CD68-positive round cells with or without CD204 positivity (Figure 2) in the lamina propria. In the lamina propria of the GB in the control group, αSMA was also expressed in vascular smooth muscle cells, but low levels of αSMA expression were found in the spindle-shaped cells. Similarly, few CD204-positive round cells were detected in the lamina propria of the GB in the control and cholecystitis groups.

Figure 3a shows the frequency of αSMA-positive cells. The percentage of cells expressing αSMA in the cancerous part (stroma) of the GB in patients with concurrent GB cancer and PBM was significantly higher than that in the lamina propria of the GB

in all patients with PBM (with and without GB cancer) as well as in the non-cancerous part (lamina propria) of the GB in patients with concurrent GB cancer and PBM ($P < 0.05$). There was no significant difference in the number of αSMA-positive cells between the lamina propria of the GB in patients with PBM and the non-cancerous part (lamina propria) of the GB in patients with concurrent GB cancer and PBM ($P = 0.2771$). Additionally, the PBM group showed more αSMA-positive cells in the lamina propria of the GB than did the control group ($P < 0.05$) and cholecystitis group ($P = 0.057$). Figure 3b and c shows the frequency of cells expressing CD204 and CD68, respectively. Expression of CD204, an M2 macrophage marker, in the lamina propria of the GB was significantly higher in the PBM than control group ($P < 0.05$) and tended to be higher than that in the cholecystitis group ($P = 0.072$). Expression of CD68, an M1 and M2 macrophage marker, was highest in the lamina propria of the GB in the cholecystitis group and tended to be higher than that in the control group ($P = 0.055$); however, there was no significant difference among all three groups. Figure 3d shows that the CD204/CD68 ratio, which indicates the proportion of M2 macrophages, was significantly higher in the lamina propria of the GB in the PBM group than in the control and cholecystitis groups ($P < 0.05$). Additionally, there was no significant

difference in the CD204/CD68 ratio in the lamina propria of the GB in patients with PBM versus the cancerous part (stroma) and non-cancerous part (lamina propria) of the GB in patients with concurrent GB cancer and PBM.

Expression of NLRP3 and caspase 1 in the GB epithelium of patients with PBM

Figure 4 shows representative immunohistochemical staining for NLRP3 and caspase-1 expression in GB samples from patients with PBM. NLRP3 and caspase-1 were detected in the cytoplasm of cells within the GB epithelium.

Figure 5a and b shows the mean H scores of five groups: control, cholecystitis, PBM, GB cancer with PBM (cancerous part), and GB cancer with PBM (non-cancerous part). The H scores for NLRP3 were 65 ± 55, 193 ± 31, 215 ± 14, 179 ± 34, and 93 ± 29, respectively, and those for caspase 1 were 91 ± 31, 143 ± 31, 171 ± 16, 209 ± 33, and 100 ± 50, respectively. Epithelial NLRP3 expression was significantly higher in the cholecystitis, PBM, and GB cancer with PBM groups than in the control group ($P < 0.05$). Furthermore, epithelial NLRP3 expression was significantly higher in the PBM group than in the GB cancer with PBM (non-cancerous) group ($P < 0.05$).

Epithelial caspase 1 expression tended to be higher in the PBM group than in

the control group ($P = 0.06$) and was significantly higher in the GB cancer with PBM group than in the control group ($P < 0.05$).

Additionally, 15 (57.8%) of 26 GB samples in the PBM group showed epithelial hyperplasia. Six (23.1%) cases showed dysplasia, and three of these cases were combined with hyperplasia. Five (19.2%) cases showed neither epithelial hyperplasia nor dysplasia. NLRP3 expression in the normal epithelium, hyperplastic epithelium, and dysplastic epithelium (with or without hyperplasia) groups was 225 ± 26, 219 ± 19, and 220 ± 35, respectively, and caspase 1 expression was 157 ± 40, 198 ± 24, and 228 ± 37, respectively. There were no significant differences among the three groups. However, NLRP3 expression in the epithelium of the GB in patients with PBM with or without hyperplastic and dysplastic regions was higher than that in the normal epithelium of the control group. One hyperplastic region in the PBM group had significantly higher caspase 1 expression than the normal epithelium in the control group ($P < 0.05$).

Expression of NLRP3 and caspase 1 in the lamina propria of the GB in patients with PBM

In the lamina propria of the GB in patients with PBM, NLRP3 and caspase 1 expression was detected in both macrophage-like round cells and fibroblast-like spindle-shaped cells (Figure 4).

Figure 5c and d shows the expression of NLRP3 and caspase 1 in spindle-shaped cells, which were regarded as activated fibroblasts, in the control, cholecystitis, PBM, GB cancer with PBM (cancerous part), and GB cancer with PBM (non-cancerous part) groups. NLRP3 expression in these five groups was 3.0 ± 0.9, 26.8 ± 3.3, 24.4 ± 3.5, 20.7 ± 2.4, and 23.7 ± 7.0/hpf, respectively, and caspase 1 expression was 7.8 ± 3.2, 15.5 ± 3.6, 21.8 ± 2.2, 18.6 ± 3.4, and 20.3 ± 2.7/hpf, respectively. There was no difference in NLRP3 or caspase 1 expression in the lamina propria of the GB in patients with PBM versus the cancerous part (stroma) or non-cancerous part (lamina propria) of the GB in patients with concurrent GB cancer and PBM. The number of NLRP3- and caspase 1-positive spindle-shaped cells was higher in the PBM than control group ($P < 0.05$). Interestingly, regarding the distribution of NLRP3- and caspase 1-positive spindle-shaped cells in patients with PBM, we observed the likelihood that some spindle-shaped cells, which expressed NLRP3 and caspase 1, existed near epithelial cells, which highly expressed both molecules (Figure 6).

Conversely, few cells that did not express these molecules were detected near the epithelium.

We next performed dual immunofluorescence staining of GB tissue from patients with PBM. We detected both NLRP3 and caspase-1 expression in activated fibroblasts, which were identified as αSMA-positive cells, in the lamina propria of the GB in patients with PBM (Figure 7).

DISCUSSION

In this study, we found high infiltration of αSMA-positive activated fibroblasts and CD204-positive M2 macrophages in the lamina propria of the GB in patients with PBM. Additionally, NLRP3 and caspase-1 expression was elevated not only in the epithelium but also in fibroblasts in patients with PBM. These data suggest that infiltration of activated fibroblasts and M2 macrophages into the lamina propria of the GB in patients with PBM is comparable to that observed in patients with GB cancer and might be related to PBM-associated biliary carcinogenesis, possibly through crosstalk of NLRP3 activation between epithelial and stromal cells.

Regarding the role of stromal cells in carcinogenesis, some studies have revealed that stromal changes also occur in healthy tissues and progressively evolve to a neoplastic state, contributing to malignant transformation of epithelial cells [6-8]. Infiltration of both activated fibroblasts and M2 macrophages has been reported as a preneoplastic state of the pancreas in patients with chronic pancreatitis [15]. In terms of the effect of activated fibroblasts on carcinogenesis, a major role of crosstalk between senescent breast luminal cells and activated fibroblasts has been suggested in promoting the inflammatory/carcinogenic microenvironment via a senescence-associated secretory

phenotype in an interleukin (IL)-8-dependent manner [8]. Regarding the link between M2 macrophages and carcinogenesis, Kvorjak et al. [6] reported that M2 macrophages might contribute to regulation of MUC1 glycosylation, a specific event during malignant transformation in colitis-associated colon cancer. Swangphon et al. [7] reported that a high density of infiltrating $CD163^+$ monocytes was associated with the severity of human papillomavirus-infected cervical lesions. Furthermore, Xue et al. [15] reported infiltration of M2 macrophages and pancreatic stellate cells into the pancreatic tissue of patients with chronic pancreatitis, indicating a neoplastic state of pancreatic cancer. The authors stated that crosstalk between these two stromal cell types via the secretion of cytokines, such as IL-4 and IL-13, might contribute to pancreatic fibrosis progression. [15] In our study, the number of CD204-positive macrophages in the lamina propria of the GB was higher in the PBM group than in the control and cholecystitis groups, and it was not significantly different regardless of the presence of GB cancer in patients with PBM. However, the number of CD68-positive macrophages was most substantially increased in patients with cholecystitis. These data suggest that proinflammatory M1 macrophages are increased in cholecystitis because of the inflammatory status of the GB tissue. Similarly, our study revealed infiltration of M2 macrophages and activated

fibroblasts into the lamina propria of the GB in patients with PBM, suggesting the role of these cells in the malignant transformation of the epithelium in patients with PBM.

NLRP3 is involved in innate immunity, and its activation has been identified in various pathological conditions, including myocardial ischemia and fibrosis [16, 17]. A relationship among NLRP3, carcinogenesis, and cancer progression was recently demonstrated [9-11,18]. Son et al. [18] reported elevation of NLRP3 expression in the colonic epithelium of patients with colitis and colitis-associated colon cancer and suggested that once tumor formation is initiated, NLRP3 inflammasome-induced IL-1β and IL-18 modulate immunity in the TME and promote cancer progression. In the biliary epithelium of patients with PBM, the incidence and degree of hyperplasia are characteristic [19]. These changes lead to a hyperplasia–dysplasia–carcinoma sequence that differs from the sequence in sporadic biliary tract cancer [19]. *K-ras* gene mutations, which are related to PBM carcinogenesis, have been observed not only in the cancerous region of patients with PBM but also in hyperplastic epithelia of the biliary tract of patients who have PBM without cancer [19,20]. In our study, NLRP3 expression in the GB epithelium of patients with PBM either with or without hyperplastic and dysplastic regions, and even in one patient in the PBM group without hyperplastic or dysplastic

regions, was higher than that in the normal epithelium of the control group. Therefore, this finding suggests that NLRP3 activation is a relatively very early step in PBM carcinogenesis.

Regarding the pro-cancerous role of NLRP3 in activated fibroblasts, Ershaid et al. [11] reported tumor-promoting functions of CAFs in breast cancer in sensing tumor-induced tissue damage, including releasing damage-associated molecular patterns (DAMPs) and activating the NLPR3 inflammasome pathway, which promotes tumor progression and metastasis. NLRP3 activation in M2 macrophages is also reportedly involved in cancer migration [21]. However, no report has examined whether NLRP3 activation in stromal cells influences carcinogenesis. In our study, activation of the NLRP3 inflammasome was detected in patients with PBM, not only in the GB epithelium but also in the GB lamina propria (especially in activated fibroblasts), compared with the control group. Additionally, NLRP3- and caspase 1-positive activated fibroblasts and M2 macrophages were distributed immediately beneath the relative molecule-positive epithelium. This result suggests crosstalk between epithelial and stromal cells during PBM carcinogenesis. Regarding the relationship between NLRP3 activation and stromal changes, Alyaseer et al. [22] reported that the maturation of

IL-1β through NLRP3 and caspase-1 activation in epithelial cells promotes transcription of the *TGF-β* gene in an autocrine, paracrine, or endocrine manner. Because TGF-β is an indicator of CAFs, NLRP3 activation in epithelial cells might lead to CAF infiltration. Guo et al. [23] reported that the NLRP3 inflammasome/IL-1β pathway promotes the recruitment of TAMs in the TME of breast cancer. NLRP3 activation also induces pyroptosis, a proinflammatory mode of cell death. In this process, the cell membrane is ruptured and IL-1β and IL-18, inflammatory DAMPs, are released to propagate proinflammatory responses [24]. Our data suggest that NLRP3 activation affects carcinogenesis of the GB epithelium in patients with PBM. Furthermore, previous studies suggest crosstalk between epithelial and stromal cells via NLRP3 activation, TGF-β secretion, and DAMP release.

This study has two main limitations. First, we defined spindle-shaped cells as fibroblasts and quantified the number of NLRP3- and caspase 1-positive cells. However, several types of cells other than fibroblasts and macrophages may express these molecules, such as lymphocytes. In some reports, the total number of stromal cells was counted instead of the number of each type of cell, such as fibroblasts and macrophages; other reports used the same approach as our method, and spindle cells were defined as

fibroblasts. Thus, the number of NLRP3- and caspase 1-positive fibroblasts might have been overcounted. Additionally, the lamina propria of the cholecystitis group was very thin because of inflammation and submucosal edema. The area of the lamina propria of the GB in the cholecystitis group, in which NLRP3-positive fibroblasts were counted, was larger than that in the other groups. Although NLRP3 expression in the lamina propria of the GB in the cholecystitis group was much higher, the finding of edema in patients with cholecystitis is a possible reason, and some area corrections are needed in further studies. Second, our analysis was limited to an immunohistochemical approach. An in vitro PBM model was previously established using a cholangiocyte cell line and lysophosphatidylcholine, which is elevated in patients with PBM [25]. Metabolomics analysis of bile samples from patients with PBM in our institute also revealed lysophosphatidylcholine as a carcinogenic candidate [26]. More in vitro studies on the stromal changes during PBM carcinogenesis are needed.

In conclusion, our results show that activated fibroblasts and M2 macrophages may be associated with carcinogenesis of PBM, possibly through NLRP3 inflammasome activation.

ACKNOWLEDGMENTS

We thank Gabrielle White Wolf, PhD; Mitchell Arico; and Angela Morben, DVM, ELS from Edanz (https://jp.edanz.com/ac) for editing a draft of this manuscript.

CONFLICT OF INTEREST

Dr. M. Shimada received a research grant from Taiho Pharmaceutical Co., Ltd. No other authors have a conflict of interest.

FUNDING

This work was partly supported by a collaborative research grant from Taiho Pharmaceutical Co., Ltd. (Tokyo, Japan) and the Japan Society for the Promotion of Science KAKENHI [grant numbers 20K08957 and 21K08671].

REFERENCES

1. Morine Y, Shimada M, Takamatsu H, Araida T, Endo I, Kubota M, *et al.* Clinical features of pancreaticobiliary maljunction: update analysis of 2nd Japan-nationwide survey. J Hepatobiliary Pancreat Sci. 2013; **20**(5):472-80.
2. Matsubara T, Sakurai Y, Zhi LZ, Miura H, Ochiai M, Funabiki T. K-ras and p53 gene mutations in noncancerous biliary lesions of patients with pancreaticobiliary maljunction. J Hepatobiliary Pancreat Surg. 2002; **9**(3):312-21.
3. Tokuda K. Morine Y, Miyazaki K, Yamada S, Saito Y, Nishi M, *et al.* The interaction between cancer associated fibroblasts and tumor associated macrophages via the osteopontin pathway in the tumor microenvironment of hepatocellular carcinoma. Oncotarget., 2021; **12**(4):333-343.
4. Chen S, Morine Y, Tokuda K, Yamada S, Saito Y, Nishi M, *et al*. Cancer-associated fibroblast-induced M2-polarized macrophages promote hepatocellular carcinoma progression via the plasminogen activator inhibitor-1 pathway. Int J Oncol. 2021; **59**(2):59.
5. Hashimoto O, Yoshida M, Koma Y, Yanai T, Hasegawa D, Kosaka Y, *et al*. Collaboration of cancer-associated fibroblasts and tumour-associated macrophages

for neuroblastoma development. J Pathol., 2016; **240**(2):211-23.

6. Kvorjak M. Ahmed Y, Miller ML, Sriram R, Coronnello C, Hashash JG, *et al*. Cross-talk between Colon Cells and Macrophages Increases ST6GALNAC1 and MUC1-sTn Expression in Ulcerative Colitis and Colitis-Associated Colon Cancer. Cancer Immunol Res., 2020; **8**(2):167-178.

7. Swangphon P, Pientong C, Sunthamala N, Bumrungthai S, Azuma M, Kleebkaow P, *et al*. Correlation of Circulating $CD64^{+}$/$CD163^{+}$ Monocyte Ratio and stroma/peri-tumoral $CD163^{+}$ Monocyte Density with Human Papillomavirus Infected Cervical Lesion Severity. Cancer Microenviron 2017; **10**(1-3):77-85.

8. Al-Khalaf HH, Ghebeh H, Inass R, Aboussekhra A. Senescent Breast Luminal Cells Promote Carcinogenesis through Interleukin-8-Dependent Activation of Stromal Fibroblasts. Mol Cell Biol. 2019; **39**(2):e00359-18.

9. Karki R. Kanneganti TD. Diverging inflammasome signals in tumorigenesis and potential targeting. Nat Rev Cancer. 2019; **19**(4):197-214.

10. Yu S. Yin JJ, Miao JX, Li SG, Huang CZ, Huang N, *et al*. Activation of NLRP3 inflammasome promotes the proliferation and migration of esophageal squamous cell carcinoma. Oncol Rep. 2020; **43**(4):1113-1124.

11. Ershaid N. Sharon Y, Doron H, Raz Y, Shani O, Cohen N, *et al*. NLRP3 inflammasome in fibroblasts links tissue damage with inflammation in breast cancer progression and metastasis. Nat Commun. 2019; **10**(1):4375.

12. Morine Y. Imura S, Ikemoto T, Iwahashi S, Saito Y, Shimada M. CD44 Expression Is a Prognostic Factor in Patients with Intrahepatic Cholangiocarcinoma After Surgical Resection. Anticancer Res. 2017; **37**:5701-5705.

13. Nakagawa M, Karim MR, Izawa T, Kuwamura M, Yamate J. Immunophenotypical Characterization of M1/M2 Macrophages and Lymphocytes in Cisplatin-Induced Rat Progressive Renal Fibrosis. Cells. 2021; 10(2):257.

14. Ogawa H, Azuma M, Uehara H, Takahashi T, Nishioka Y, Sone S, et al. Nerve growth factor derived from bronchial epithelium after chronic mite antigen exposure contributes to airway hyperresponsiveness by inducing hyperinnervation, and is inhibited by in vivo siRNA. Clin Exp Allergy. 2012; 42(3):460-470.

15. Xue J. Sharma V, Hsieh MH, Chawla A, Murali R, Pandol SJ, *et al*. Alternatively activated macrophages promote pancreatic fibrosis in chronic pancreatitis. Nat Commun. 2015; **6**:7158.

16. Kawaguchi M. Takahashi M, Hata T, Kashima Y, Usui F, Morimoto H, *et al*. Inflammasome activation of cardiac fibroblasts is essential for myocardial ischemia/reperfusion injury. Circulation. 2011; **123**(6):594-604.

17. Artlett CM. The Role of the NLRP3 Inflammasome in Fibrosis. Open Rheumatol J. 2012; **6**:80-6.

18. Son HJ. Sohn SH, Kim N, Lee HN, Lee SM, Nam RH, *et al*. Effect of Estradiol in an Azoxymethane/Dextran Sulfate Sodium-Treated Mouse Model of Colorectal Cancer: Implication for Sex Difference in Colorectal Cancer Development. Cancer Res Treat. 2019; **51**(2):632-648.

19. Funabiki T, Matsubara T, Miyakawa S, Ishihara S. Pancreaticobiliary maljunction and carcinogenesis to biliary and pancreatic malignancy. Langenbecks Arch Surg. 2009; **394**(1):159-69.

20. Tanno S, Obara T, Fujii T, Mizukami Y, Shudo R, Nishino N, et al. Proliferative potential and K-ras mutation in epithelial hyperplasia of the gallbladder in patients with anomalous pancreaticobiliary ductal union. Cancer. 1998; **83**(2):267-75.

21. Zhang Q. Wang H, Mao C, Sun M, Dominah G, Chen L, *et al*. Fatty acid oxidation contributes to IL-1β secretion in M2 macrophages and promotes

macrophage-mediated tumor cell migration. Mol Immunol. 2018; **94**:27-35.

22. Alyaseer AAA, de Lima MHS, Braga TT . The Role of NLRP3 Inflammasome Activation in the Epithelial to Mesenchymal Transition Process During the Fibrosis. Front Immunol. 2020; **11**:883.

23. Guo B, Fu S, Zhang J, Liu B, Li Z. Targeting inflammasome/IL-1 pathways for cancer immunotherapy. Sci Rep. 2016; **6**:36107.

24. Kayagaki N, Dixit VM. Rescue from a fiery death: A therapeutic endeavor. Science. 2019; **366**(6466):688-689.

25. Shimizu R, Kanno K, Sugiyama A, Ohata H, Araki A, Kishikawa N, *et al.* Cholangiocyte senescence caused by lysophosphatidylcholine as a potential implication in carcinogenesis. J Hepatobiliary Pancreat Sci. 2015; **22**(9):675-82.

26. Mori H, Morine Y, Mawatari K, Chiba A, Yamada S, Saito Y, *et al*. Bile Metabolites and Risk of Carcinogenesis in Patients With Pancreaticobiliary Maljunction: A Pilot Study. Anticancer Res. 2021; **41**(1):327-334.

FIGURE LEGENDS

Figure 1. Immunostaining staining of αSMA in the lamina propria of the gallbladder.

Spindle-shaped cells positive for αSMA were seen in the lamina propria of the gallbladder of patients with PBM (×400 magnification). Conversely, few positively stained cells were detected in the lamina propria of the gallbladder in the control group.

PBM: pancreaticobiliary maljunction

Figure 2. Dual immunofluorescence of CD204 and CD68 in gallbladder tissue.

Round cells positive for CD204/68 were found in the lamina propria of the gallbladder in patients with PBM. Conversely, few positively stained cells were detected in the lamina propria of the gallbladder in the control and cholecystitis groups.

Arrow: CD204/68 double-positive cell, PBM: pancreaticobiliary maljunction

Figure 3. Quantification of immunohistochemical staining.

(a) αSMA, (b) CD204, (c) CD68, and (d) ratio of CD204/CD68 expression.

*$P < 0.05$, GB: gallbladder, PBM: pancreaticobiliary maljunction

Figure 4. Immunostaining for NLRP3 and caspase 1 in gallbladder tissue.

(a) NLRP3 (400× magnification). (b) Caspase 1 (400× magnification). Macrophage-like round cells are shown by black arrows and fibroblast-like spindle cells by arrows. NLRP3- and caspase 1-positive activated fibroblasts (arrowhead) were distributed immediately beneath the relative molecule-positive epithelium.

NLRP3: Nod-like receptor pyrin domain containing 3

Figure 5. Quantification of immunohistochemical staining for NLRP3 and caspase 1 in the epithelium and stroma.

(a) NLRP3 (H-score) and (b) caspase 1 (H-score) in the epithelium. (c) NLRP3 (cell number) and (d) caspase 1 (cell number) in the stroma.

*P < 0.05, GB: gallbladder, PBM: pancreaticobiliary maljunction, NLRP3: Nod-like receptor pyrin domain containing 3

Figure 6. Distribution of NLRP3 and caspase 1-positive stromal cells in PBM.

(a) NLRP3. (b) Caspase 1.

+1 and 2 are intensity scores in the H-score evaluation.

NLRP3: Nod-like receptor pyrin domain containing 3, PBM: pancreaticobiliary maljunction

Figure 7. Dual immunofluorescence staining of gallbladder tissue in PBM.

(a) NLRP3 (green) and αSMA (red). (b) Caspase 1 (green) and αSMA (red). Arrows indicate NLRP3- or caspase 1-positive activated fibroblasts.

NLRP3: Nod-like receptor pyrin domain containing 3.

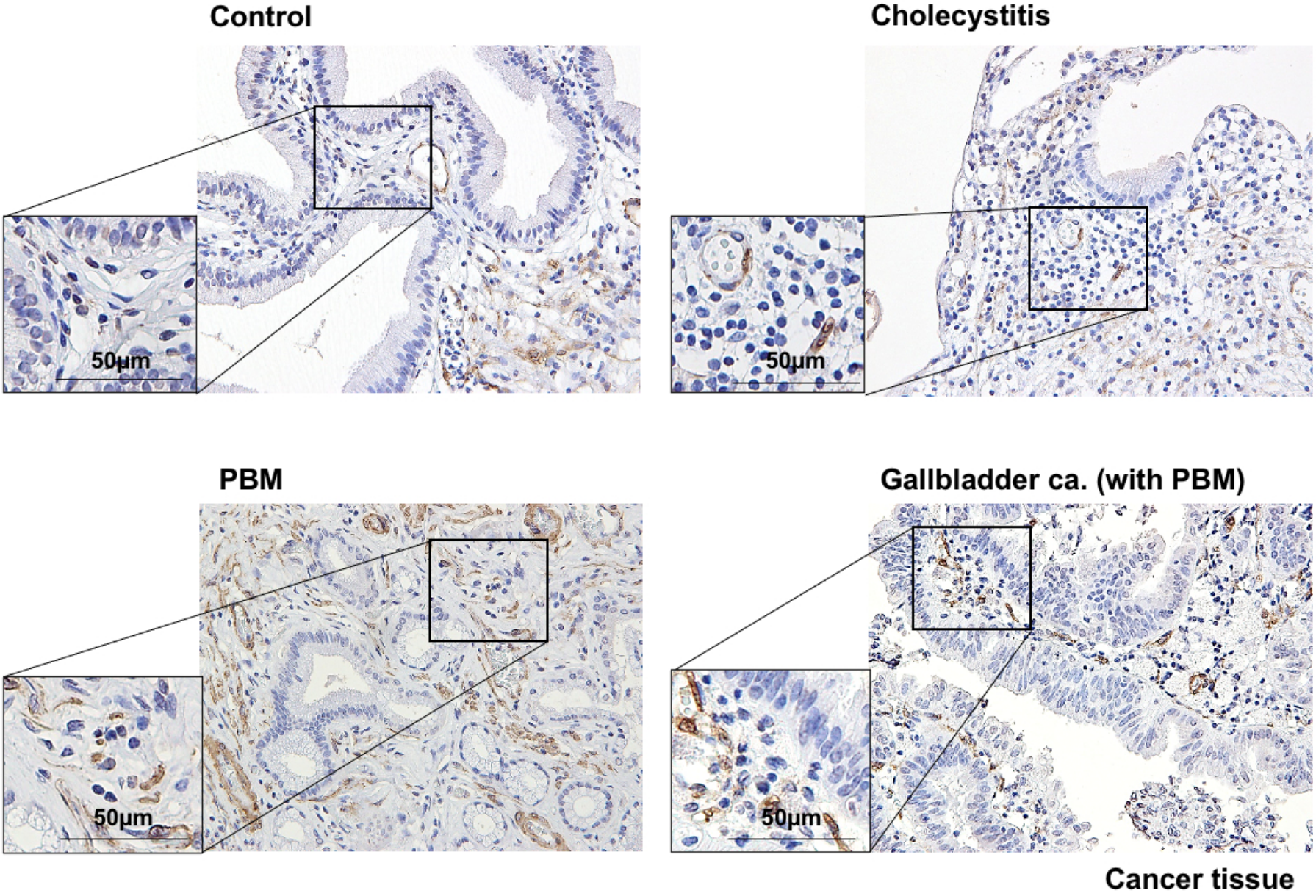
Control
50μm
Cholecystitis
50μm
PBM
50μm
Gallbladder ca. (with PBM)
50μm
Cancer tissue

Figure 1

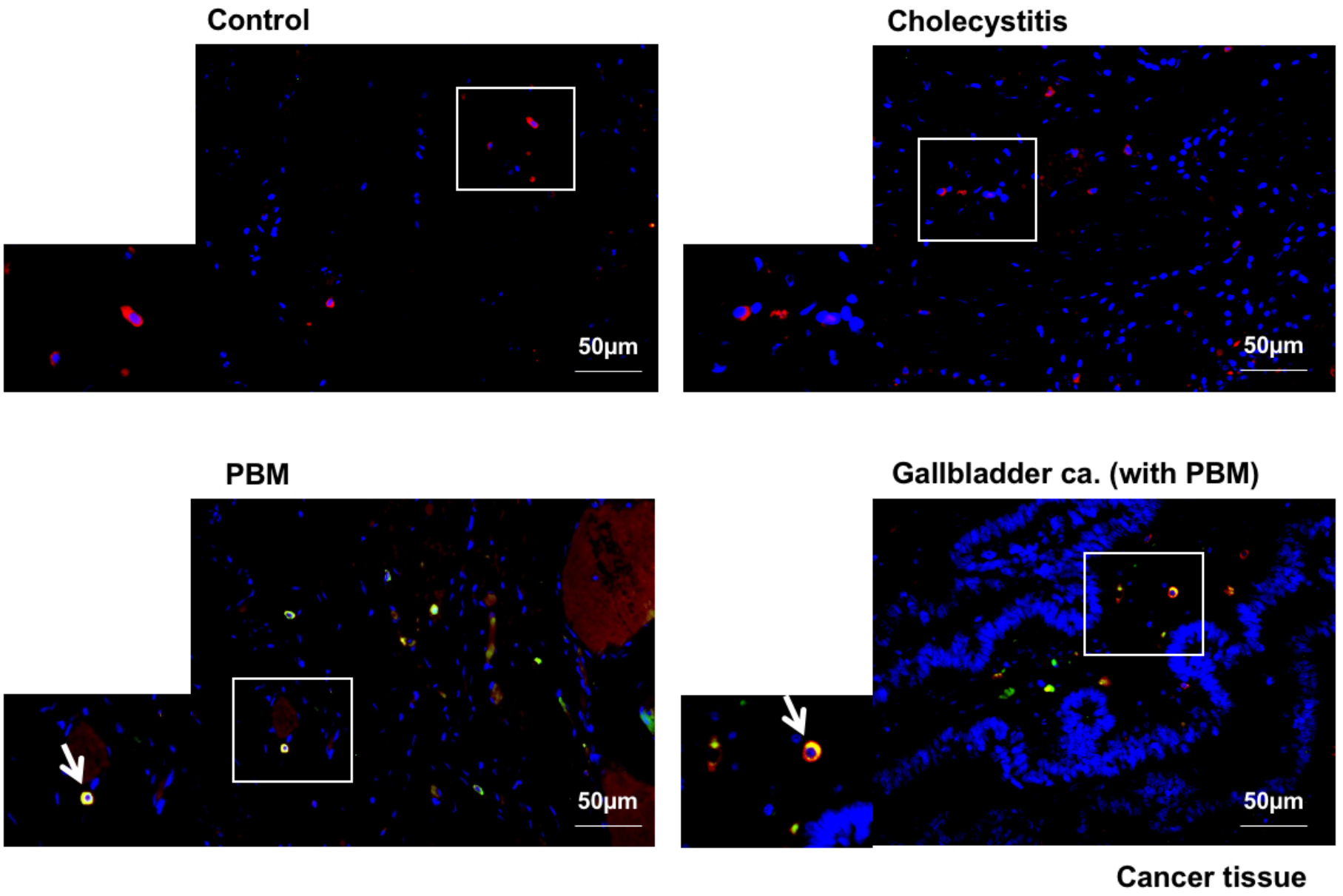
Control
50μm
Cholecystitis
50μm
PBM
50μm
Gallbladder ca. (with PBM)
50μm
Cancer tissue

Figure 2

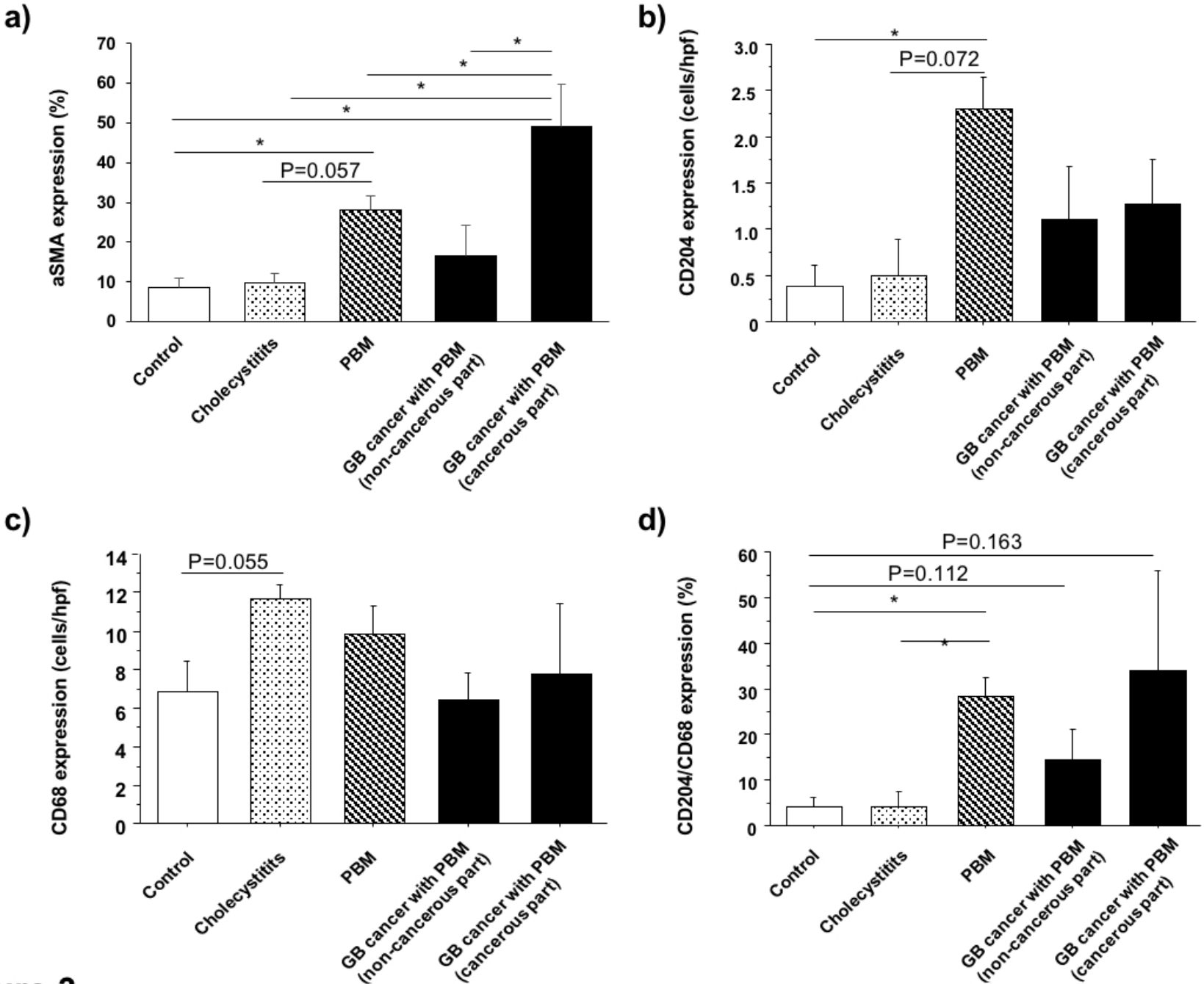
a)
aSMA expression (%)
70
60
50
40
30
20
10
0
*
*
*
*
*
P=0.057
Control
Cholecystitits
PBM
GB cancer with PBM (non-cancerous part)
GB cancer with PBM (cancerous part)
b)
CD204 expression (cells/hpf)
3.0
2.5
2.0
1.5
1.0
0.5
0
*
P=0.072
Control
Cholecystitits
PBM
GB cancer with PBM (non-cancerous part)
GB cancer with PBM (cancerous part)
c)
CD68 expression (cells/hpf)
14
12
10
8
6
4
2
0
P=0.055
Control
Cholecystitits
PBM
GB cancer with PBM (non-cancerous part)
GB cancer with PBM (cancerous part)
d)
CD204/CD68 expression (%)
60
50
40
30
20
10
0
P=0.163
P=0.112
*
*
Control
Cholecystitits
PBM
GB cancer with PBM (non-cancerous part)
GB cancer with PBM (cancerous part)

Figure 3

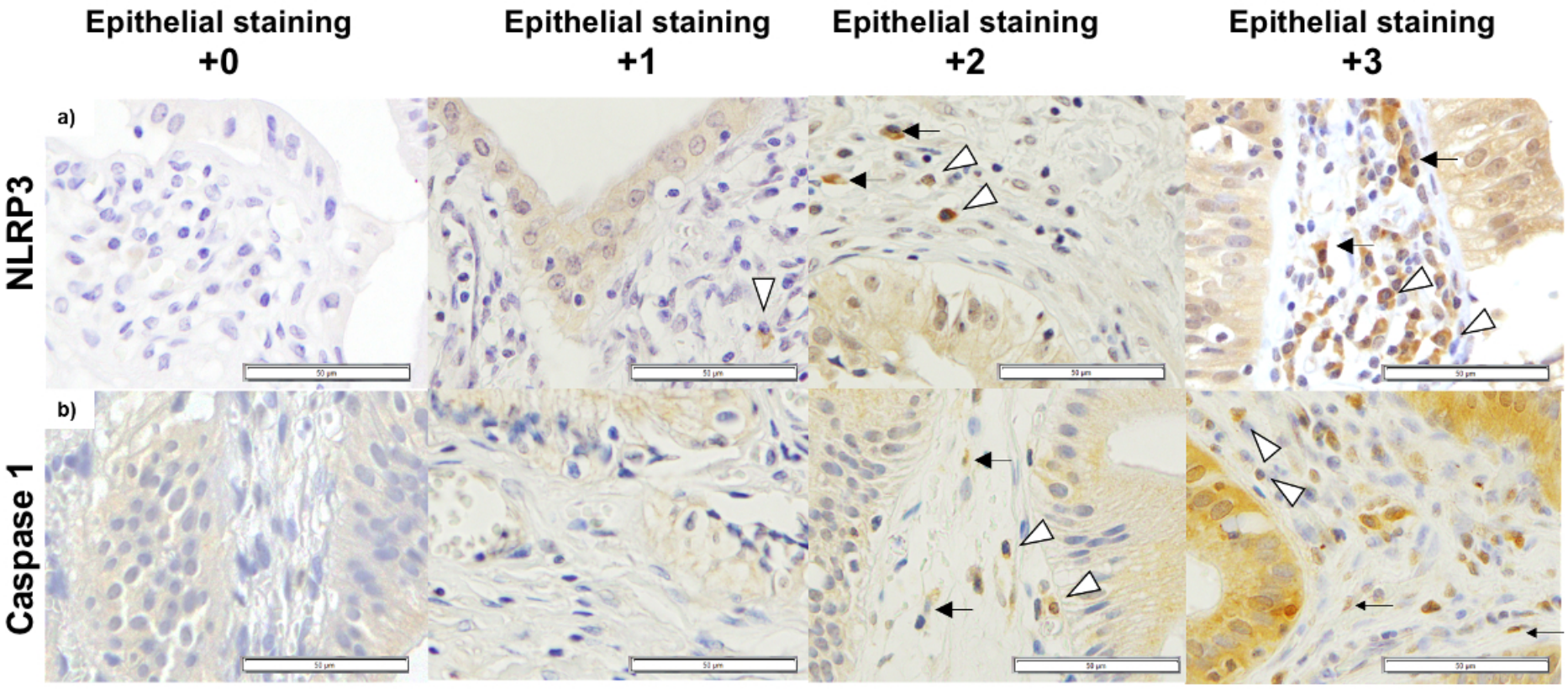
Epithelial staining
+0
Epithelial staining
+1
Epithelial staining
+2
Epithelial staining
+3
a)
NLRP3
b)
Caspase 1

Figure 4

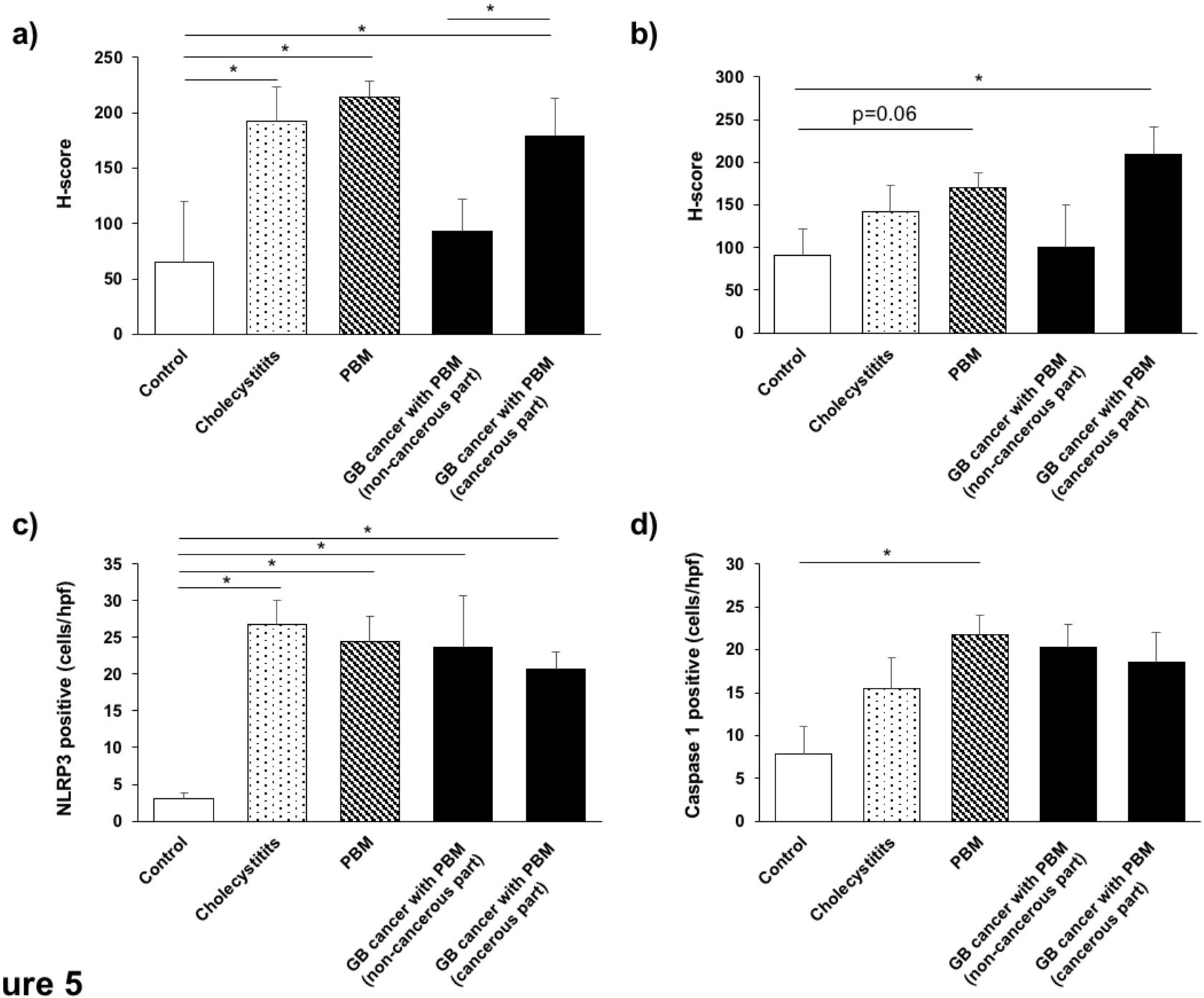
a)
H-score
250
200
150
100
50
0
*
*
*
*
*
Control
Cholecystitits
PBM
GB cancer with PBM (non-cancerous part)
GB cancer with PBM (cancerous part)
b)
H-score
300
250
200
150
100
50
0
*
p=0.06
Control
Cholecystitits
PBM
GB cancer with PBM (non-cancerous part)
GB cancer with PBM (cancerous part)
c)
NLRP3 positive (cells/hpf)
35
30
25
20
15
10
5
0
*
*
*
*
*
Control
Cholecystitits
PBM
GB cancer with PBM (non-cancerous part)
GB cancer with PBM (cancerous part)
d)
Caspase 1 positive (cells/hpf)
30
25
20
15
10
5
0
*
Control
Cholecystitits
PBM
GB cancer with PBM (non-cancerous part)
GB cancer with PBM (cancerous part)

Figure 5

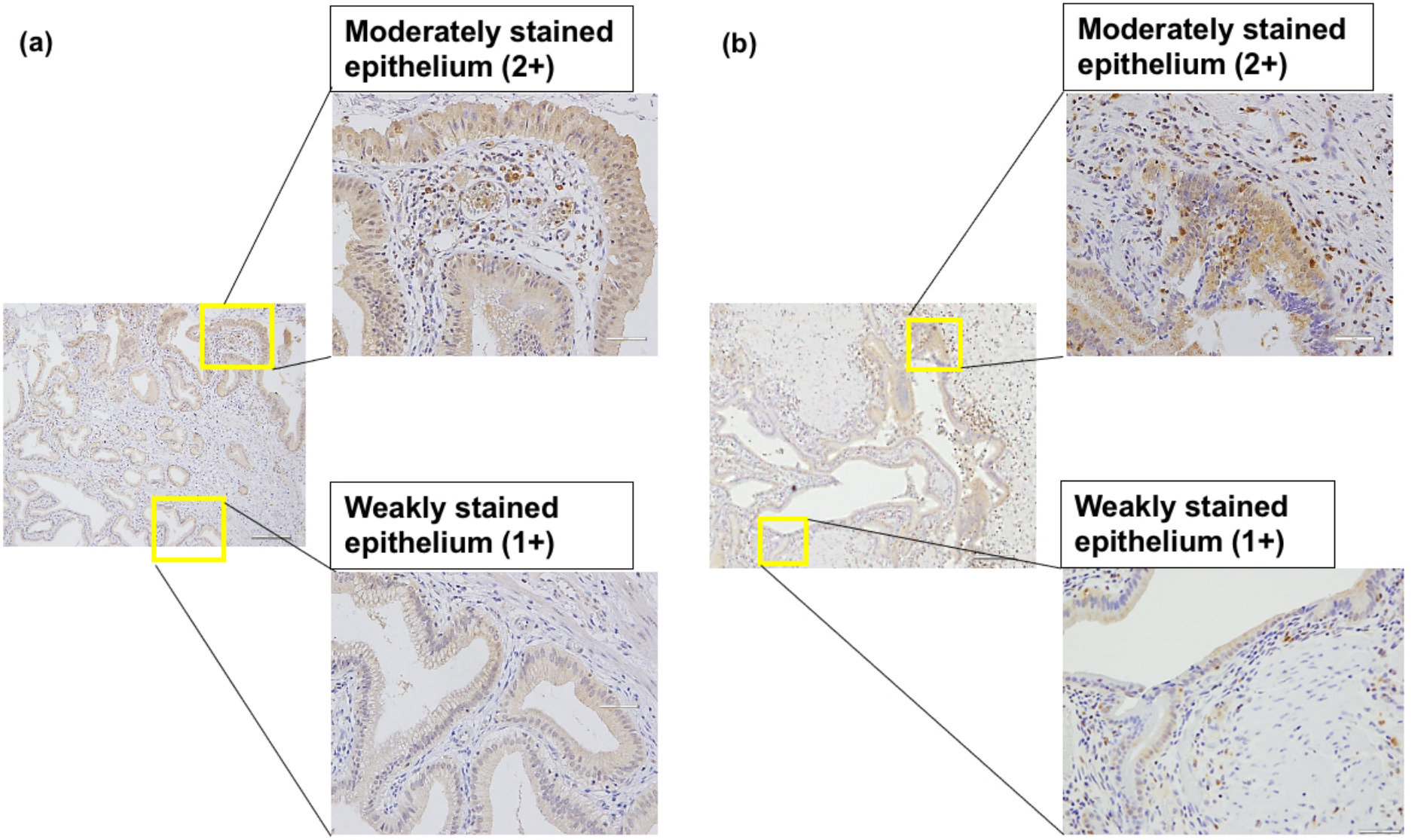
(a)
Moderately stained epithelium (2+)
Weakly stained epithelium (1+)
(b)
Moderately stained epithelium (2+)
Weakly stained epithelium (1+)

Figure 6

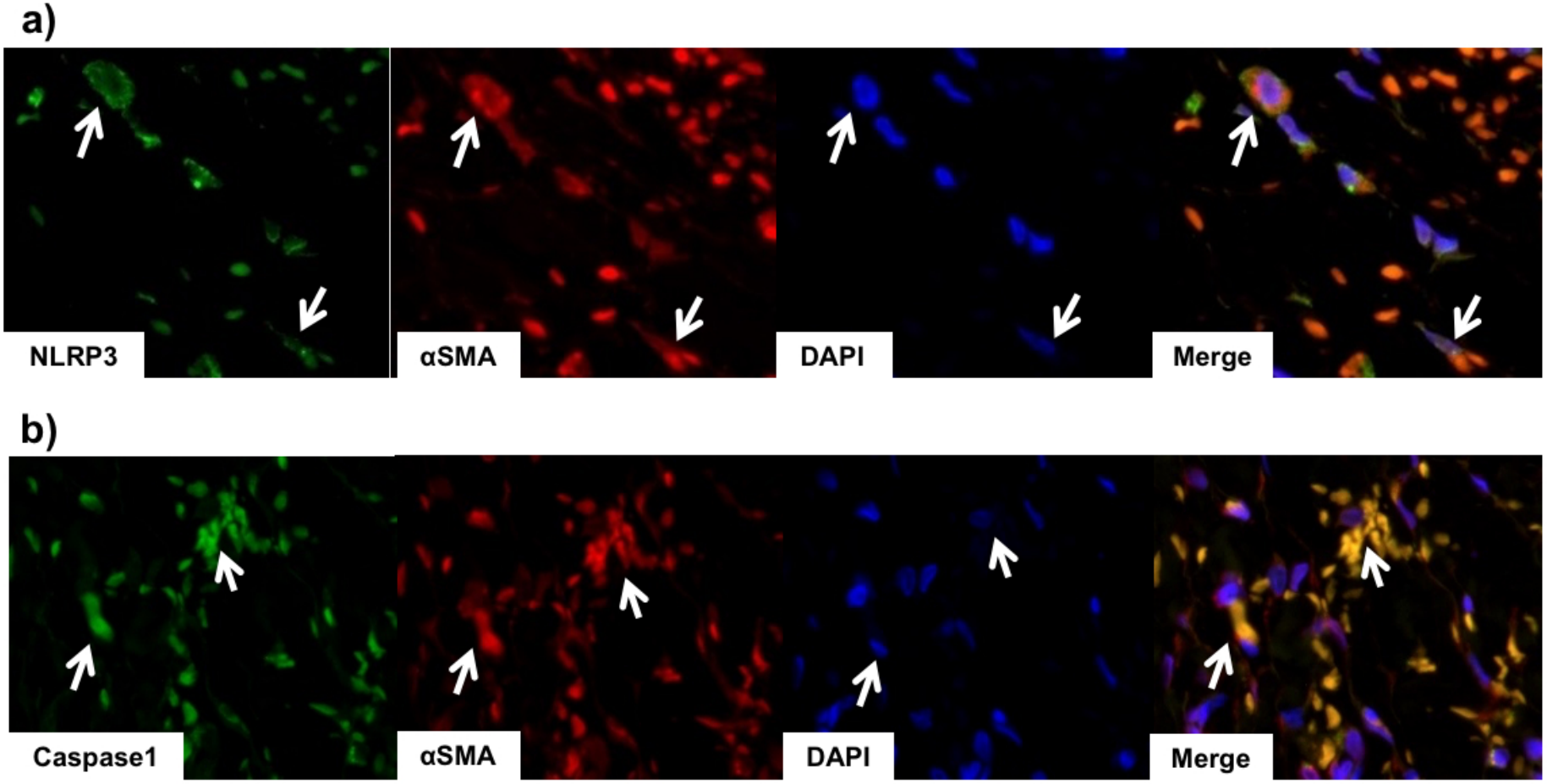

Figure 7